ROCKY MOUNTAIN
JOURNAL OF MATHEMATICS
Volume 7, Number 3, Summer 1977

COEXISTENCE OF STABLE AND RANDOM MOTION

R. C. CHURCHILL, G. PECELLI, S. SACOLICK, AND D. L. ROD*

0. **Introduction.** Stable and pathological phenomena, the latter as in the Smale horseshoe map, have been extensively studied in the theory of dynamical systems. However, the present authors are unaware of any explicit example where both of these phenomena occur simultaneously. This paper presents such an example where the interlinked stability and pathology occur on a fixed energy surface of a Hamiltonian system of two degrees of freedom. In particular, we show that on "many" energy surfaces in our example one has both a pair of linked periodic orbits that are elliptic stable (and hence encased in invariant tori), and interlinking pathological solutions "generated" from the (topological) transversal intersection of the stable and unstable manifolds of four distinct hyperbolic periodic orbits. The example has been extensively studied in [8, 3, 4, 5, and 12] and should be contrasted with an example of Easton [6] which exhibits linked hyperbolic periodic orbits giving rise to a pathological structure.

To demonstrate the elliptic stability of our periodic orbits we use results from the theory of Mathieu equations [1, 9, 10] to show that the eigenvalues of the linearized Poincaré maps about these orbits move along the unit circle as the total energy h of the Hamiltonian system changes. This allows us to choose h so that certain eigenvalue conditions needed to assert stability for the full (non-linear) Poincaré map are satisfied. Thus, either the Birkhoff normal form of the Poincaré map is linear and we can apply a result of Rüssmann [13], or it is not, in which case the results of Arnold-Moser [11, p. 56] apply to assert stability. As a corollary we have the existence of quasi-periodic motion in a system which we show is in no sense near an integrable one. Such solutions are usually obtained by perturbing from an integrable Hamiltonian.

For the pathology we use numerical work to verify the conditions necessary to apply the results in [4, 5], the hyperbolicity of the relevant periodic orbits having been shown in [12]. These techniques for constructing invariant tori and establishing pathology are relevant to other problems (in particular the breakdown of invariant tori) as we shall indicate in a discussion of the Hénon-Heiles Hamiltonian in § 5.

Received by the editors on November 3, 1976.
*Author supported in part by National Research Council of Canada, Grant #A8507.

We remark that E. Zehnder has shown that the coexistence of stable and random motion is generic for elliptic symplectic planar mappings fixing the origin (see [15] or [11, pp. 105–106]). However, the pathology in his case is a consequence of the ellipticity, and occurs in any neighborhood of the origin. In our example the pathology is bounded away from the stable periodic orbits.

1. **The Example.** We study the Hamiltonian system

$$\dot{x}_i = \partial H/\partial y_i, \quad \dot{y}_i = -\partial H/\partial x_i, \quad i = 1, 2, \tag{1.1}$$

where $H(x, y) = (1/2)(y_1^2 + y_2^2) + (1/2)(x_1^2 + x_2^2) - (1/2)x_1^2 x_2^2$, $x = (x_1, x_2)$, $y = (y_1, y_2)$. The Hill's region for $H(x, y) = h > 1/2$ is given in Figure 1 (the shading will be explained below), where the appropriate portions $\underline{w}_1, \underline{w}_2$, of the x_1 and x_2-axes are projections of two periodic orbits w_1, w_2, that are linked in phase space (these are the elliptic stable orbits). Let $W(x) = (1/2)(x_1^2 + x_2^2) - (1/2)x_1^2 x_2^2$ be the potential function. We will denote the x-plane projection of sets and orbits in phase space by underlining.

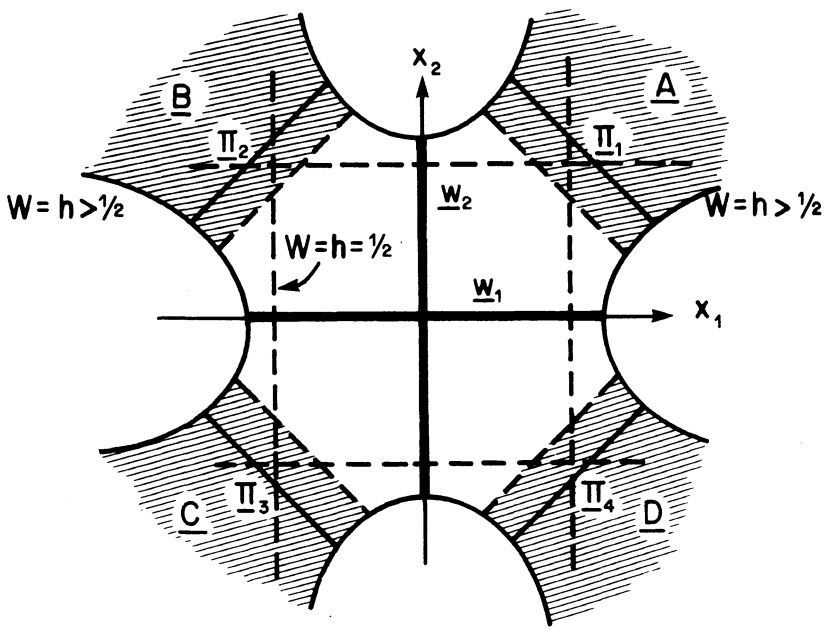

Figure 1

A topological model of the phase space is given in Figure 2, where the vertices and lateral surfaces of the double solid cone are identified as indicated by identifying points p and q if p is vertically above q. (This can be shown by using the fact that above every point x in the plane there is a "circle of velocities" $\{(x, y) : |y|^2 = 2[h - W(x)]\}$ in phase space with radius that goes to zero on the boundary $W(x) = h$ of the Hill's region.) The four open 3-balls A, B, C, D, that have been removed project to the shaded portions of Figure 1, and for energies $(1/2 < h \leqq (9/2)$ each contains a single hyperbolic periodic orbit Π_i of energy h whose projection Π_i joins the boundaries $W(x) = h$ of the corresponding leg [12, § 4, Ex. D] (see Fig. 1).

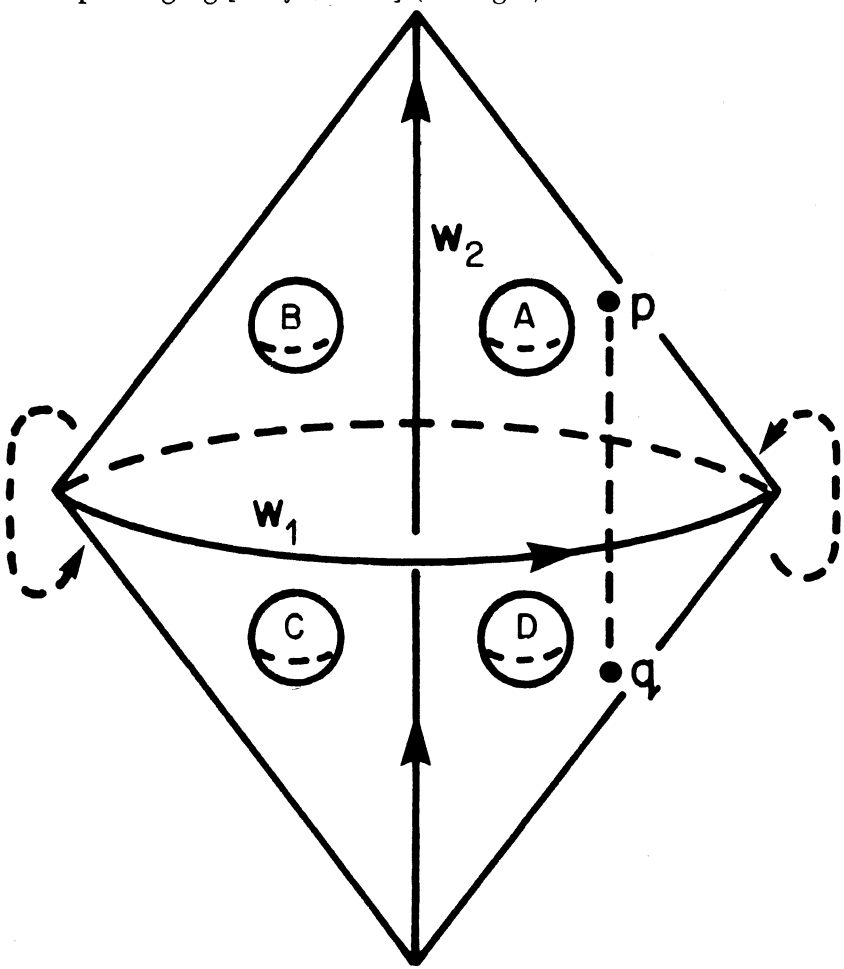

Figure 2

We will show that for almost all energies h near .99, w_1 and w_2 are enclosed in invariant tori which nest down on these orbits, and that the following pathology exists [5, Theorems 1.3, 1.4, and 7.2]:

(a) Given any bi-infinite sequence of the letters A, B, C, D, in which no letter repeats itself, there are uncountably many solutions of (1.1) which pass through the open 3-balls in the prescribed order;

(b) given any finite sequence of these letters, there are uncountably many solutions of (1.1) which come from infinity in the leg corresponding to the first letter, pass from region to region in the prescribed order, and return to infinity in the leg indicated by the last letter;

(c) given any finite sequence with identical first and last letters, there is a nonempty subset of the solutions of (1.1) that can be analyzed using the shift operator on a space of bi-infinite sequences of finitely many letters, and for each integer $l > 0$ there is a periodic orbit which passes through the regions in the prescribed order l times and then closes;

(d) there is no second integral G of (1.1) with $G \mid \Pi_i = c_i$ and (h, c_i) as a regular value of $(H, G) : R^4 \to R^2$ for the energies h near .99 which we use below.

In the next two sections we concentrate on showing the existence of the invariant tori.

2. **The Eigenvalues of the Linearized Poincaré Map.** For all energies $h > 0$ the functions

$$w_1(t) = (2h)^{1/2}(\sin(t), 0, \cos(t), 0),$$

$$w_2(t) = (2h)^{1/2}(0, \sin(t), 0, \cos(t)),$$

are the solutions of (1.1) with total energy $H(w_i(t)) \equiv h$ drawn in Figures 1 and 2. We will compute the linearized Poincaré map along w_1, the one along w_2 having the same character by symmetry.

Linearizing around $w_1(t)$ we are led to

$$\dot{z} = \begin{pmatrix} 0 & I \\ -I & 0 \end{pmatrix} H_{**}(w_1(t))z, \quad z = \begin{pmatrix} z_1 \\ z_2 \\ z_3 \\ z_4 \end{pmatrix}, \tag{2.1}$$

where $I = \begin{pmatrix} 1 & 0 \\ 0 & 1 \end{pmatrix}$ and $H_{**} = \begin{pmatrix} W_{xx} & 0 \\ 0 & I \end{pmatrix}$ is the Hessian of H. In particular, (2.1) becomes

$$\dot{z} = \begin{pmatrix} 0 & 0 & 1 & 0 \\ 0 & 0 & 0 & 1 \\ -1 & 0 & 0 & 0 \\ 0 & -(1 - 2h \sin^2(t)) & 0 & 0 \end{pmatrix} z \tag{2.2}$$

which is equivalent to the system of second order equations

$$\ddot{z}_1 + z_1 = 0, \tag{2.3}$$

$$\ddot{z}_2 + (1 - 2h \sin^2(t))z_2 = 0. \tag{2.4}$$

Letting n_1 and n_2 be the *normalized* solutions of (2.4) satisfying $n_1(0) = 1 = \dot{n}_2(0)$ and $\dot{n}_1(0) = 0 = n_2(0)$, the fundamental matrix solution Z of (2.2) satisfying $Z(0) = I_4$ takes the value

$$Z(2\pi) = \begin{pmatrix} 1 & 0 & 0 & 0 \\ 0 & n_1(2\pi) & 0 & n_2(2\pi) \\ 0 & 0 & 1 & 0 \\ 0 & \dot{n}_1(2\pi) & 0 & \dot{n}_2(2\pi) \end{pmatrix}$$

and is the linearized Poincaré map along $w_1(t)$ calculated at one full period [7, pp. 251–253]. The area-preserving character of the Hamiltonian flow implies $\det\begin{pmatrix} n_1 & n_2 \\ \dot{n}_1 & \dot{n}_2 \end{pmatrix}_{2\pi} = 1$. Letting $\Delta = n_1(2\pi) + \dot{n}_2(2\pi)$, we see that the characteristic polynomial $\det[Z(2\pi) - \lambda I_4] = (\lambda - 1)^2(\lambda^2 - \Delta\lambda + 1)$ has two eigenvalues $\lambda = 1$ reflecting the fact that the Poincaré map is computed along the periodic orbit and on the surface $H(x, y) = h$. The remaining two eigenvalues are calculated from

$$(\lambda^2 - \Delta\lambda + 1) = 0, \tag{2.5}$$

and thus depend only on the solutions of (2.4) which can be rewritten (letting $z = z_2$)

$$\ddot{z} + [(1 - h) + h \cos(2t)]z = 0, \tag{2.6}$$

a special case of the two real parameter Mathieu equation [**10**, p. 131]

$$\ddot{z} + [\gamma - 2\delta \cos(2t)]z = 0, \quad \gamma = (1 - h), \delta = (-h/2). \tag{2.7}$$

Some elementary identities (see [9, pp. 6–8] or [**10**, § 2.12]) show that the solutions of (2.5) are given by

$$\lambda = [n_1(\pi) \pm ([n_1(\pi)]^2 - 1)^{1/2}]^2 . \tag{2.8}$$

Recalling that the Hill discriminant $\Delta_H = n_1(\pi) + \dot{n}_2(\pi) = 2n_1(\pi)$, we see that $|\Delta_H| > 2$ implies that $w_1(t)$ is a hyperbolic periodic orbit, and $|\Delta_H| < 2$ implies that it is elliptic. Plots of the $\Delta_H =$ constant curves in the (δ, γ)-plane can be found in [1, pp. 123 and 130] and [10, p. 132]. In particular, there is a lower boundary curve $a_0 = a_0(\delta)$ for the first stability region (in the interior of which $|\Delta_H| < 2$) where $a_0(\delta) \leqq 0$ and $a_0(\delta) = 0$ only for $\delta = 0$ (see Fig. 3). The upper boundary of the first stability region is depicted in Figure 3. The slopes $s(\delta)$ of each of these boundary curves satisfy $|s(\delta)| < 2$ [10, p. 133]. This gives the following result.

THEOREM 2.1. *$w_1(t)$ is an elliptic periodic orbit for $0 < h < 1 - a_0(-h/2)$, and is hyperbolic for $h > 1 - a_0(-h/2)$. Further, there exists a unique $h_0 > 0$ such that $h_0 = 1 - a_0(-h_0/2)$ and $h_0 > 1$ ($h_0 \simeq 1.15$). As h increases from 0 to h_0, the eigenvalues λ from (2.5) travel monotonically along the unit circle, both taking the value $+1$ at $h = h_0$.*

PROOF. Plotting the line $\gamma = (1 - h)$, $\delta = (-h/2)$ (thus $\gamma = 2\delta + 1$) in the (δ, γ)-plane for $h \geqq 0$ as in Fig. 3, the theorem follows from standard results and an examination of the stability chart (see [10, pp. 131–133] or [1, pp. 122–130]). In particular, the line $\gamma = 2\delta + 1$ has slope 2 which is greater than the slope of the curves $\Delta_H =$ constant and is thus transverse to them. This forces the eigenvalues λ to travel monotonically along the unit circle as h increases from 0 to h_0.

3. **The Existence of Invariant Tori.** Let $P = P(x_2, y_2)$ be the Poincaré map along $w_1(t)$, dP the linearized map $\left(\begin{smallmatrix} n_1 & n_2 \\ \dot{n}_1 & \dot{n}_2 \end{smallmatrix}\right)_{2\pi}$ calculated in the previous section. Then P and dP map the origin of R^2 to itself, hence $P(x_2, y_2) = dP\binom{x_2}{y_2} +$ (higher order terms in x_2, y_2). For energies $0 < h < h_0 \simeq 1.15$, Theorem 2.1 states that the eigenvalues λ and $\bar{\lambda}$ of dP lie on the unit circle with $\lambda \neq \pm 1$, hence $(x_2, y_2) = (0, 0)$ is an elliptic fixed point of the area-preserving mapping P. We consider only energies h in this range for which the eigenvalue $\lambda = e^{2\pi i\theta}$ has θ badly approximable by rationals (such λ form a set of full measure 2π on the unit circle). Then P can be transformed by a *formal* power series $C = C(x_2, y_2)$ into Birkhoff normal form [14, Section 23]. If the normal form is *linear*, then C is a *convergent* power series by a result of Rüssmann [13]. In this case P is conjugate to a rotation and thus $(x_2, y_2) = (0, 0)$ is a *stable* elliptic fixed point. Hence $w_1(t)$ is encased in invariant tori that nest to $w_1(t)$. If, however, the Birkhoff normal form is *not* linear, then using the first non-vanishing term in [11, Theorem 2.13], we obtain the same result on stability.

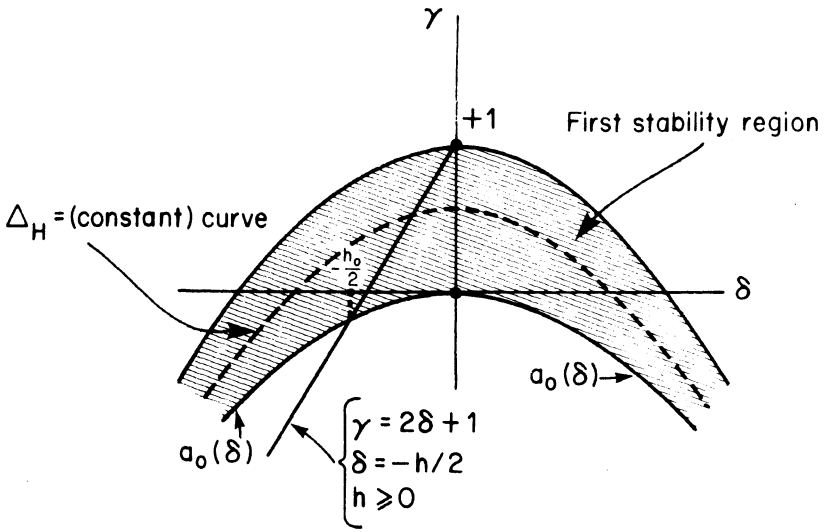

Figure 3

In either case the set of invariant tori about $w_1(t)$ has nonzero measure, and $w_1(t)$ is elliptic stable for a set of energies of full measure in $(0, h_0)$, namely those energies giving rise to eigenvalues $\lambda = e^{2\pi i\theta}$ with θ badly approximable by rationals.

4. **The Existence of Pathology.** By Theorem 7.2 of [5], the pathology given in (a)-(d) of § 1 will exist at all energies *near* $h = .99$ provided there is a "crossing orbit" *at* $h = .99$ (thereby giving such "crossing orbits" at energies near $h = .99$). That is, a solution of (1.1) is required which enters the central region from infinity in one leg in Figure 1 and departs to infinity via an adjacent (non-opposite) leg. Given one such orbit, one can use symmetry to construct crossing orbits from a given leg to any other leg. In [5, Theorem 7.2] it is shown how the existence of such crossing orbits "forces" the (topological) transversal intersection of the stable and unstable manifolds of any pair of the hyperbolic periodic orbits Π_i in the legs (see Fig. 1). The Π_i were shown to be hyperbolic in [12, § 4, Ex. D]. In essence one then has (topologically) "non-degenerate" heteroclinic orbits (see [4, § 5] for definition) connecting distinct hyperbolic periodic orbits, and this enables one to "essentially" embed the horseshoe may into the flow.

In [5] the difficulties involved in showing the existence of crossing orbits are described in detail, and for the example under consideration such orbits were only proven to exist at energy $h = 3$, although they were also found numerically at $h = 2$, 1.5, and 1.25. The proof in [5] involves an error analysis of the computed crossing orbit to show that it represents an actual solution of (1.1). Unfortunately, for the lower energies the motion was too slow to control the exponential growth with time of the error estimates. Thus, modifications were required in the computer program outlined in [5, § 3 and 5] to prove the existence of the crossing orbit found at $h = .99$ which is schematically indicated in Fig. 4.

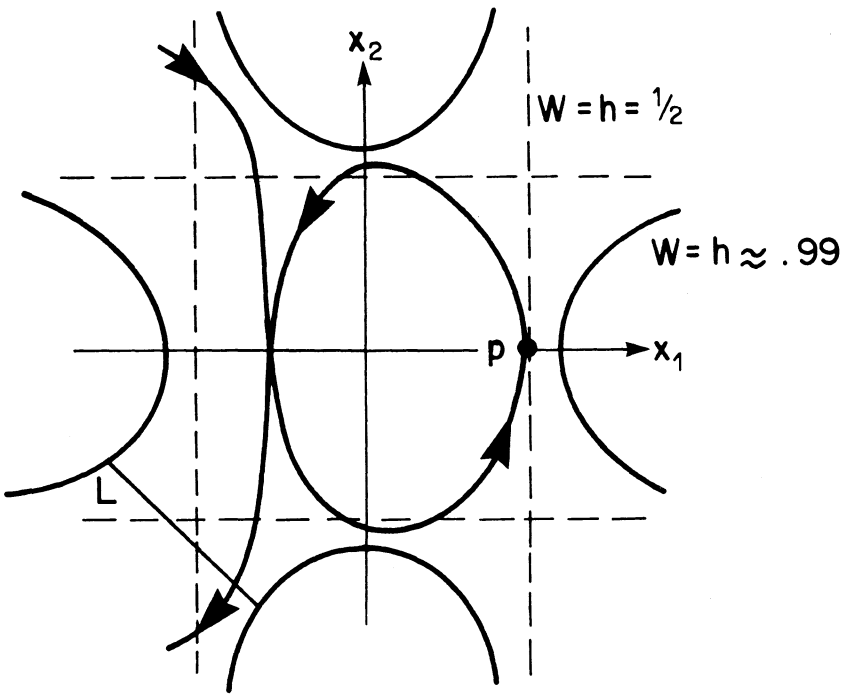

Figure 4

Before discussing these modifications we summarize: for energies h near .99 we see that the crossing orbit condition in [5] for pathology is satisfied simultaneous to the eigenvalue condition required to assert the existence of invariant tori about $w_i(t)$, $i = 1, 2$. We thus have the coexistence of stable and random motion at such energies.

The computer program for numerical integration of the crossing

orbit followed in outline [5, § 3 and 5]. At energy $h = .99$ the initial conditions were $x = (1, 0)$, $y = (0, (.98)^{1/2})$ thereby starting the orbit at p in Figure 4 with velocity perpendicular to the x_1-axis. The computed orbit moved forward, and by symmetry backwards, as indicated. Due to the values of the acceleration field $-W_x$, one needs only to show that the orbit goes somewhat to the left of the "minimum distance" line segment L between the two branches of the level curve $W(x) = h = .99$. Thus one needs error bounds only up to this point (see [5, § 3 and 5] for more detail; in particular, Fig. 27).

The fourth order Taylor series used in [5] for numerical integration was insufficient to control the truncation error over the relevant time interval in the present example. Therefore a computerized symbolic (non-arithmetic) differentiation scheme was utilized to provide Taylor series of unrestricted order. The final analysis used an eleventh order series with timestep $\Delta = 10^{-2}$, and the total truncation error was of the order of 10^{-7}.

Unfortunately, double precision was insufficient to control the roundoff error when the eleventh order series was used. Further refinements led to using the extended precision floating-point feature of the *PL*1 optimizing compiler of the IBM 360-370, which has a mantissa representation of 112 significant binary digits. The final roundoff error was then bounded by 10^{-15}.

As opposed to [5], where manual error estimates were done, the current program was designed to calculate the truncation and roundoff errors in addition to computing the solution. This was done by first computing the orbit and then repeating the calculations to do the error analysis. In order to eliminate any effect of machine error in the error bound calculations themselves, the program rounded *up* after each arithmetical operation so as to truly bound the truncation and roundoff errors. For the same purpose we generously overestimated the bounds of a region in the phase space containing the computed orbit. This region corresponds to the region R^* in [5, § 5], and is the region on which the error bounds were calculated.

It should be remarked that the solution computed with a fourth order Taylor series and double precision did not differ significantly from the final computed solution, but as already mentioned the latter method with eleventh order series had to be used to bound the errors. Just as a check we calculated the total energy along the computed solution, and found it constant through the 25th decimal place.

ADDENDUM: The versatility and additional precision of the current program led to a check on certain crossing orbits for the Hénon-Heiles

potential which were found numerically in [5, § 6] but could not be proved to exist due to lack of appropriate error bounds. It has now been confirmed that the orbits for that potential previously found at energies $h = 7/24$ and $h = 19/80$ do represent actual crossing orbits, and thus the pathology of solutions for that potential must exist at these energies.

5. **Remarks on a Related Example.** We study the Hénon-Heiles Hamiltonian

$$H(x, y) = (1/2)(y_1^2 + y_2^2) + W(x), \tag{5.1}$$

with potential $W(x) = (1/2)(x_1^2 + x_2^2) + (1/3)x_1^3 - x_1x_2^2$, at energies $0 < h < 1/6$. The Hamiltonian studied in [2, 8] can be transformed to (5.1) by a trivial canonical transformation. The differential equations associated with (5.1) have three gradient line solutions whose projections $G_i(t)$, $i = 1, 2, 3$, are given in Figure 5.

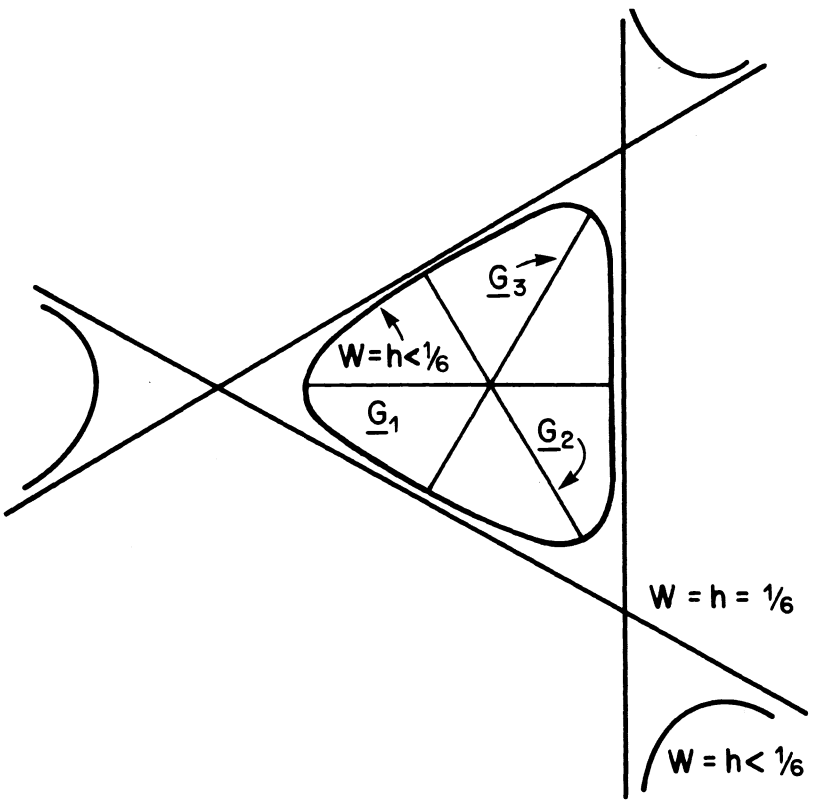

Figure 5

In [2] M. Braun established the existence of invariant tori in this Hamiltonian at energies h close to 0. His techniques also apply to our example above [2, p. 313], but only at energies too low to be useful to us. On the other hand, the techniques of the present paper applied to the $G_i(t)$ would provide invariant tori in the Hénon-Heiles Hamiltonian at those energies at which the required eigenvalue conditions are satisfied. Unfortunately, the integration of the linearized Poincaré map around $G_1(t)$, and calculation of its eigenvalues, requires a detailed knowledge of the stability chart for a Hill's equation with elliptic function coefficients (a Lamé equation). Initial numerical studies indicate that $G_1(t)$ is elliptic for $0 < h < .13$ and $.16 < h < 1/6$, but hyperbolic for $.13 < h < .16$ (as sampled at energy intervals of $\Delta h = 10^{-2}$). The numerical studies of Hénon and Heiles [8], however, indicate that pathology first appears at $h \simeq .11$ before $G_1(t)$ bifurcates to become hyperbolic. Thus it appears that this example also has coexistence of stable and random motion in the energy range $.11 < h < .13$. Considered as a model for invariant torus breakdown, the example of the present paper leads to interesting conjectures in the Hénon-Heiles Hamiltonian relating the onset of pathology to the bifurcation to transversal intersection of the stable and unstable manifolds of distinct hyperbolic orbits which one can readily locate in the diagrams of [8], and easily construct in Figure 5.

References

1. F. M. Arscott, *Periodic Differential Equations*, Pergamon Press, Oxford, 1964.

2. M. Braun, *On the applicability of the third integral of motion*, J. Differential Equations 13 (1973), 300–318.

3. R. C. Churchill, G. Pecelli and D. L. Rod, *Isolated unstable periodic orbits*, J. Differential Equations 17 (1975), 329–348.

4. R. C. Churchill and D. L. Rod, *Pathology in dynamical systems* I: *General theory*, J. Differential Equations 21 (1976), 39–65.

5. ——, *Pathology in dynamical systems* II: *Applications*, J. Differential Equations 21 (1976), 66–112.

6. R. Easton, *Isolating blocks and symbolic dynamics*, J. Differential Equations 17 (1975), 96–118.

7. P. Hartman, *Ordinary Differential Equations*, John Wiley, New York, 1964.

8. M. Hénon and C. Heiles, *The applicability of the third integral of motion: Some numerical experiments*, Astronom. J. 69 (1964), 73–79.

9. W. Magnus and S. Winkler, *Hill's Equation*, Interscience, New York, 1966.

10. J. Meixner and F. W. Schaefke, *Mathieusche Funktionen und Sphaeroid Funktionen*, Springer, Berlin, 1954.

11. J. Moser, *Stable and Random Motions in Dynamical Systems*, Annals of Mathematics Studies, No. 77, Princeton University Press, Princeton, N.J., 1973.

12. D. L. Rod, G. Pecelli and R. C. Churchill, *Hyperbolic periodic orbits,* to appear in J. Differential Equations.

13. H. Rüssman, *Über die Normalform analytischer Hamiltonscher Differentialgleichungen in der Nähe einer Gleichgewichtslösung,* Math. Annalen **169** (1967), 55-72.

14. C. L. Siegel and J. K. Moser, *Lectures on Celestial Mechanics,* Springer, New York, 1971.

15. E. Zehnder, *Homoclinic points near elliptic fixed points,* Comm. Pure Appl. Math. **26** (1973), 131-182.

HUNTER COLLEGE, CUNY, NEW YORK, NEW YORK 10021
UNIVERSITY OF CALGARY, CALGARY, ALBERTA, CANADA T2N IN4